The Eurasia Proceedings of Science, Technology, Engineering & Mathematics (EPSTEM)
ISSN: 2602-3199

The Eurasia Proceedings of Science, Technology, Engineering & Mathematics (EPSTEM), 2022

Volume 21, Pages 335-348

IConTES 2022: International Conference on Technology, Engineering and Science

Study of the Correlation between the Process Parameters and the Mechanical Characteristics of the Aluminum Sheets Welded by the FSW Process

Mohamed MERZOUG
Liabes University of Sidi-Bel-Abbes

Abdelatif MIMMI
Djillali Liabes University of Sidi-Bel-Abbes

Abdelkader GHAZI
Mustapha Stambouli University of Mascara

Abstract: In recent years, friction stir welding (FSW) methods have been used to obtain good joint mechanical and process properties. The development of FSW for lap joint manufacturing will expand the number of applications that can benefit from this technology. The objective of the present work is to the modeling of parameters influencing the temperature during friction stir lap welding joints. The area of physical understanding is the influence of the tool pin geometry and material on the temperature field, microstructural refinement, resulting material flow, and the influence of flow variations on the subsequent mechanical properties of FSW butt lap joints in aluminum 3003 Alloy. The results obtained allowed us to propose a mathematical model to study the interactions between different factors. Thus, it was shown that the most influential parameters are respectively the rotation speed and weld speed. The study also presents the influence of different parameters welding on the structure of lap joints. The hardness in the welded region is significantly lower with respect to the base material. The fracture shows the characteristics of ductile-brittle mixed fracture.

Keywords: Friction stir welding, Lap joint, Aluminum 3003, Temperature, Tensile shear test, Predicting

Introduction

Friction stir welding (FSW) is a relatively new welding process that may have significant advantages compared to the fusion processes as follow: joining of conventionally non-fusion weldable alloys, reduced distortion and improved mechanical properties of weldable alloys joints due to the pure solid-state joining of metals (Chen et al., 2003). In this process, the heat is originally derived from the friction between the welding tool (including the shoulder and the probe) and the welded material, which causes the welded material to soften at a temperature less than its melting point (Threadgill et al., 2009; Mishra et al., 2005; Xue et al., 2011; Barekatain et al., 2014; Wiedenhoft et al., 2018; Naik et al., 2013). FSW can also assemble different joint configurations, such as lap, butt, and T-joints, of which the lap joints are widely applied in vehicle and aircraft design and manufacturing. Of importance for friction stir lap welding (FSLW), how- ever, is the greater diligence necessary in developing and optimizing tool designs and process parameters to break the surface oxide layer on two planar surfaces and mitigate the three main defects, i.e., kissing bonds, hooking, and top workpiece thinning (Naik et al., 2013).

Aydin et al., (2017), studied the effect of welding parameters (rotation speed and welding speed) on the mechanical properties of 3003-H12 aluminum alloy joints produced by friction stir welding where the weld strength increased with increasing the welding speed or decreasing the rotation speed. To produce the best weld quality these parameters have to be determined for each component and alloy.

The effectiveness of these parameters on the properties of friction stir welds as well as the realization of their influence on the properties of the weld are the subject of studies carried out by several researchers (Aydin, 2010; Balasubramanian, 2014; Elangovan & Balasubramanian, 2007; Buffa et al., 2006). A great number of studies have been focused on the determine the microstructural and mechanical properties of the joints of heat treatable 3XXX aluminum alloys (Birol & Kasman, 2013a; Birol & Kasman, 2013b; Tutar et al., 2014). This last is the alloy which has been widely used purpose alloys for moderate-strength applications requiring good workability, such as stampings, spun and drawn parts and products, chemical equipment, storage tanks, fan blades, walk ways, flooring, and truck and trailer components (Tutar et al., 2014).

The object of this paper is to develop and high mechanical properties for AA3003 during friction stirs lap welding. The Design of Experiments technique was applied for the modeling and prediction of the behavior of the friction stir-welded joint. Response surface method (RSM) has been used to develop the model. In addition, this optimization allows the development of experimental results and may help to better understand the complexity of the phenomena resulting from contact parts/tool during the stirring process.

Materials and Method

The materials used were AA 3003 alloys of 2 mm thickness. Samples were cut according to the shape shown in the figure 1. The external sheets were welded parallel to the rolling direction while the central sheet was put in the long transverse direction for FSW process in order to limit potential effect of rolling texture. The chemical composition of the aluminum 3003 sheet is presented in Table1 and the mechanical properties of the sheets are presented in Table 2.

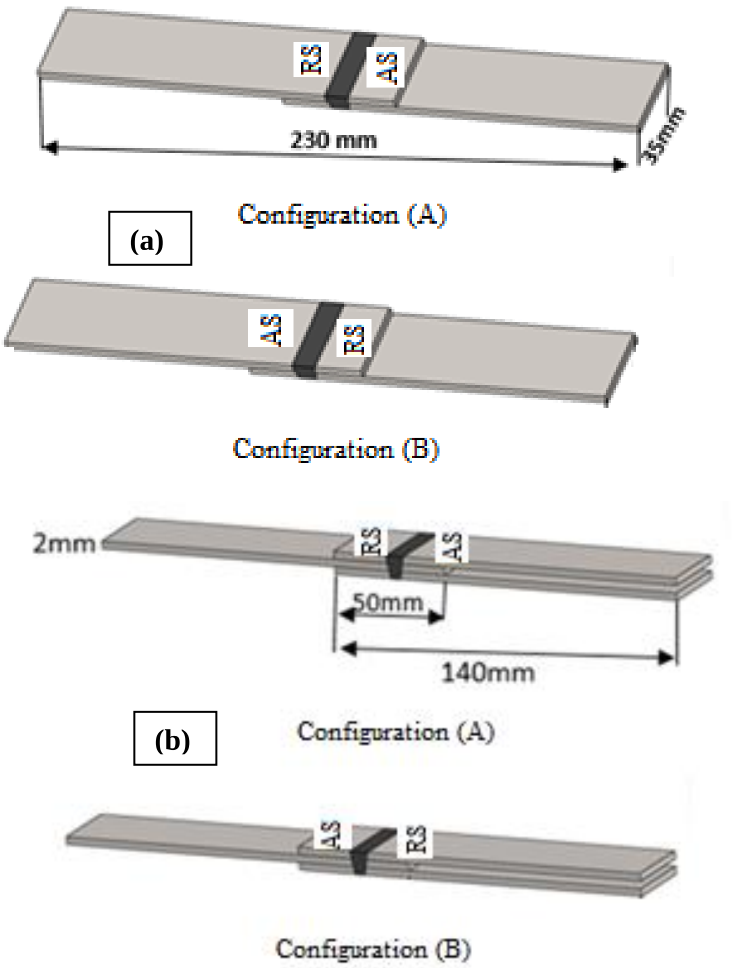

Figure1. Lap shear specimens, a) single lap, b) double lap

Table 1. Chemical composition of 3003 aluminum alloy

Element	Al	Mn	Si	Fe	Cu	Ti	Zn
%	96.7	1.3	0.9	0.9	0.13	0.1	0.3

Table 2. Mechanical properties of 3003 aluminum alloy

Rs (MPa)	UTS (MPa)	A (%)	Micro hardness (HV)	Ys (MPa)	Ym (GPa)
127	160	5.6	51	110	60

Two welding tools used for the single and double overlap joint is made of steel type 42CrMo4 (figure 2), it has the mechanical properties (Rm = 750/1300 MPa, A= 10-14 %, Re = 500/900 MPa and E = 210000 MPa). FSLW was conducted at selected rotation speeds of 1000, 1400 and 2000 rpm and selected travel speeds of 160, 200 and 250 mm/min.

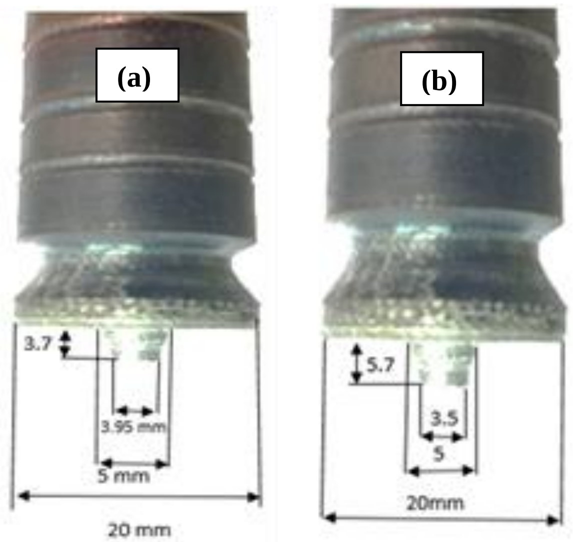

Figure 2. Geometry of the tools used, (a) single lap, (b) double lap.

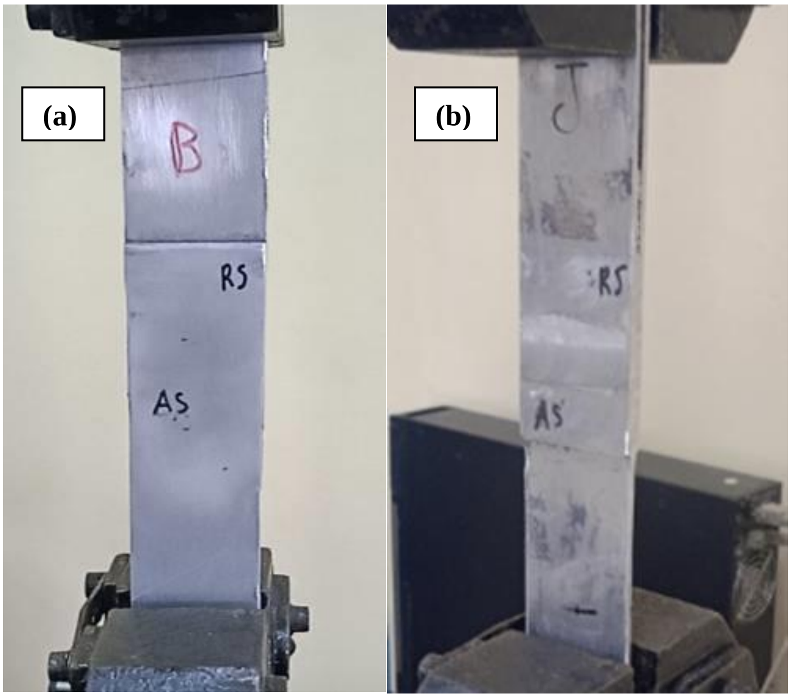

Figure 3. Overlap shear fracture testing configurations, a) single lap, b) double lap.

In this study, we conducted experiments on both formalities configuration (A) and (B) in both type's single lap and double lap on an INSTRON tensile machine at a transverse speed of 2 mm / min. The test continued until rupture will allow us to measure the ultimate elongation as shown in figure 3. The hardness on the weld cross-section was measured point wise at speeds (1400 rpm and 200 mm/min) in both forms single and double lap by shimadzu HMV-2000 micro durometer with a load 1000g and a dwell time of 10 s.

Response Surface Methodology

Analysis of variance (ANOVA) test was performed to identify the process parameters that are statistically significant. The purpose of the ANOVA test is to investigate the significance of the process parameters, which affect the temperature of FSLW joints. In addition, the rotational speeds used have a significant effect on temperature.

In order to predict the temperature during the welding operation , the response surface methodology (RSM) is used to develop the non-linear model of the FSW joints of aluminum alloys AA 3003.The response control factors for the analysis were rotation speed and welding speed. These factors and parameters were used to build up the mathematical model that could be used for prediction of the optimum factor.

Developing a Mathematical Model

Response surface methodology is a collection of mathematical and statistical techniques useful for analyzing problems in which several independent variables influence a dependent variable or response and the goal is to optimize the response. For these experimental conditions, the model used has form given below:

$$Y = \emptyset\ (x_1, x_2, \ldots\ldots\ldots\ldots\ldots\ldots, x_k) \pm e_r \qquad (1)$$

The design of experiments approach was applied to 12 tests, two replicates are considered for each combination of the input variables, which made it possible to define the coefficients summarized in Table 3.

Table 3. Results of the design of experiments

Test	Rotation speed (tr/min)	Welding speed (mm/min)	T1 Conf (A) (single lap) (°C)	T2 Conf (B) (single lap) (°C)	T1 Conf (A) (double lap) (°C)	T2 Conf (B) (doublelap) (°C)
1	1000	160	230	276	221	206
2	1400	160	225	283	241	249
3	2000	160	270	313	229	351
4	1000	200	191	295	217	198
5	1400	200	239	329	278	212
6	2000	200	274	331	283	366
7	1000	250	229	267	184	174
8	1400	250	225	327	216	184
9	2000	250	268	320	259	222
10	1400	200	239	329	278	212
11	1400	200	239	329	278	212
12	1400	200	239	329	278	212

The temperature of FSLW is a function of the welding parameters such as tool rotational speed (N) and welding speed (Sw) it can be expressed as,

Temperature = f (N, Sw).

The polynomials help optimize the temperature parameters in order to reach the desired responses. To calculate the coefficients of the models, a regression method based on the least squares criterion is used. The mathematical models suggested by MODDE 5.0 are:

$$(T_1) = 238 + 18{,}75 * rot - 0.499978 * wel + 21.25 * rot^2 - 11 * wel^2 - 0.25001 * rot * wel \quad (2)$$

$$(T_2) = 328.13 + 15{,}5798 * rot + 5.19328 * wel - 7.69192 * rot^2 - 11.3592 * wel^2 + 2.19171 * rot * wel \quad (3)$$

$$(T_3) = 273.209 + 21{,}1205 * rot - 6.49861 * wel - 8.45218 * rot^2 - 18.5031 * wel^2 + 6.50707 * rot * wel \quad (4)$$

$$(T_4) = 220.042 + 60{,}1667 * rot - 37.6667 * wel + 45.875 * rot^2 - 19.625 * wel^2 - 24.25 * rot * wel \quad (5)$$

Results and Discussion

The result of RSM design of experiment is displayed in Table 4. The residuals in figure 4 are falls on a straight line, which depicts that the errors are normally distributed (Kadaganchi et al, 2014), which reveals that there is very good correlation between the experimental value and predicted value of the responses.

Table 4. Design matrix with responses (Temperature)

Test	Rotation speed (tr/min)	Welding speed (mm/min)	T1 Conf (A) (single lap) (°C)	T2 Conf (B) (single lap) (°C)	T1 Conf (A) (double lap) (°C)	T2 Conf (B) (doublelap) (°C)
1	-1	-1	230	276	221	206
2	0	-1	225	283	241	249
3	1	-1	270	313	229	351
4	-1	0	191	295	217	198
5	0	0	239	329	278	212
6	1	0	274	331	283	366
7	-1	1	229	267	184	174
8	0	1	225	327	216	184
9	1	1	268	320	259	222
10	0	0	239	329	278	212
11	0	0	239	329	278	212
12	0	0	239	329	278	212

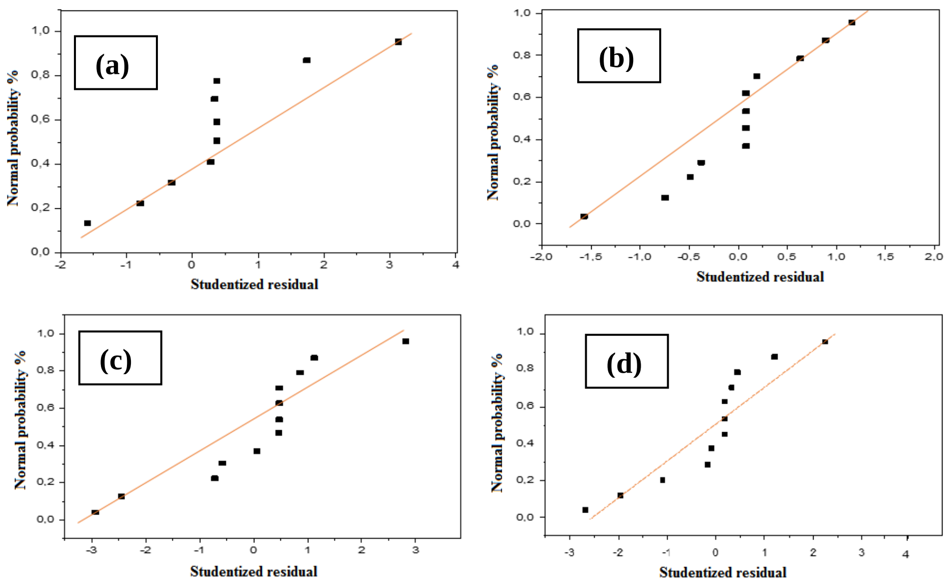

Figure 4. Normal probability plot of regression, a) configuration A (lap joint), b) configuration B (lap joint), c) configuration A (Double lap joint), d) configuration B (Double lap joint)

All the above considerations indicate an excellent adequacy of the regression models. Figure 5 shows the effect of the rotational speed and welding speed on the temperature. Experimental treatments that were conducted at different tool rotational speeds: 1000 rpm and 2000 rpm were chosen to study the effect of variation in tool rotational speed on the transient temperature distribution within the welding zone. It is noted that the temperature decreases gradually with the increasing welding speed and this is attributed by the high rotational speed results in the metallurgical transformation (figures. 5.b, 5.d, 5.f and 5.h).

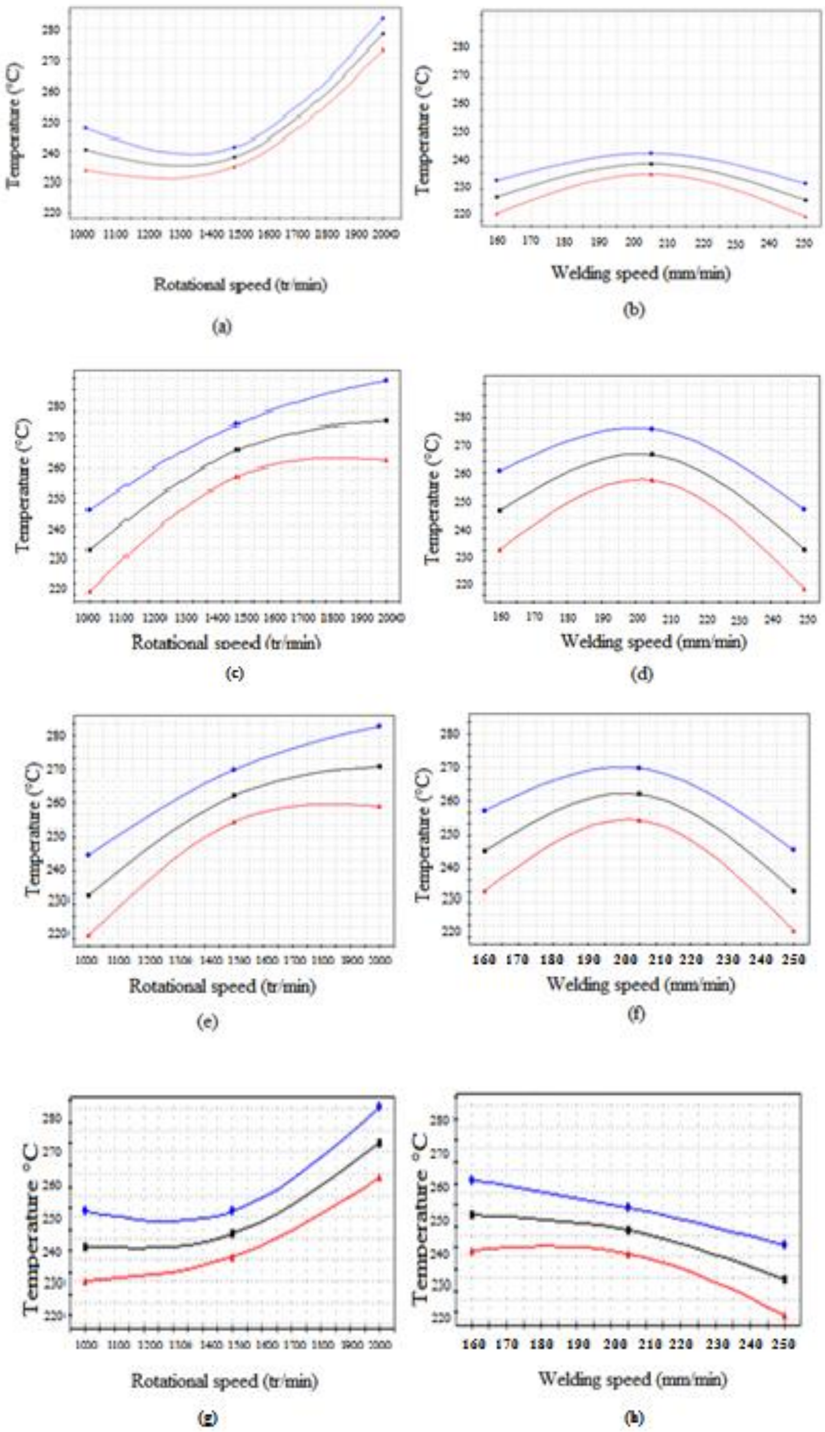

Figure 5. Analysis of thermal profile measured at the welding, a) and b) configuration A (lap joint), c) and d) configuration B (lap joint), e) and f) configuration A (Double lap joint), g) and h) configuration B (Double lap joint)

In figure (5a) maximum temperature of the experimental test that it was detected for a rotational speed of 2000 rpm was approximately 366 °C for the sample with tool speed of 200 mm/min and the minimal is detected with 1000 rpm at 184 °C. The temperature profiles have a uniform plot during the welding process which is trending symmetrically toward the peak of thermal cycles, and dropping axisymmetrically after passing through the maximum temperature.

In this analysis step, it was decided to broaden the scope of our study by taking into account the interaction between two factors. This allows viewing the output parameters on a three dimensional (3D) graph (figure 6); this graph depicts the variation of the temperature as a function of the two factors (Rotation speed and welding speed). In figure 7, it is observed that the value of the temperature was 337, 1°C at the rotational speed was 1900 rpm and the welding speed was 210 mm\min (figure 7.b), whereas the value of the temperature decreases to (272.9 °C) at the rotational speed was (2000 rpm) and the welding speed was 210 mm\min (figure.7.a). It is also observed that for the double lap joint the highest value of the temperature was 360 ° C at a rotation speed of 2000 rpm (figure.7.c) and a welding speed of 160 mm / min and decreases at 270 ° C for a rotation of 1600 rpm and a welding speed of 220 mm \ min (figure.7.d).

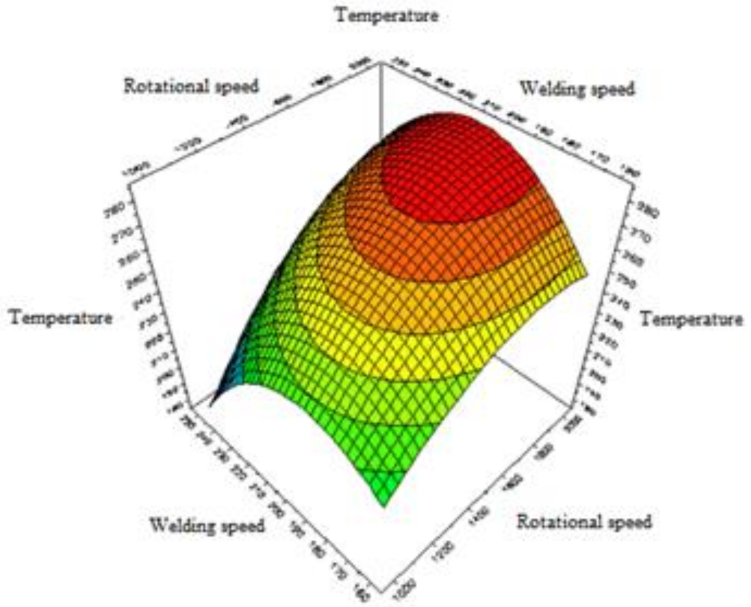

Figure 6. Three-dimensional (3D) variation of temperature as a function of rotation speed and welding speed

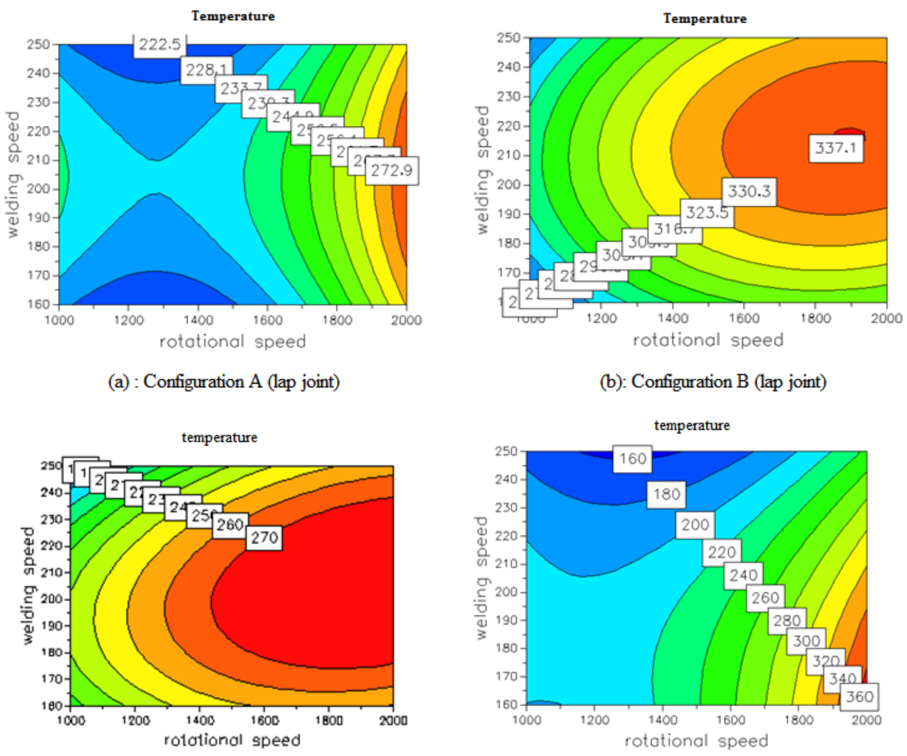

(a) : Configuration A (lap joint)

(b): Configuration B (lap joint)

(c) : Configuration A (Double lap joint)

(d): Configuration B (Double lap Joint)

Figure 7. Variation of temperature as a function of the two factors

Figure 8 shows the most influential parameters on temperature. The effects of the factors are shown using a bar graph. This diagram gives the effects in decreasing order of their importance in absolute value. This figure clearly shows the sensitivity of the rotational speed and the welding speed respectively to temperature. A small change in rotational speed causes large temperature changes as the welding speed increases. The results obtained by this study show that the temperature is more sensitive to the speed of rotation than to the speed of welding. After a thorough analysis, these figures show that the classification of the dominant factors on the maximum temperature is as follows: (rot) and (rot * rot). (figure.7a). On the other hand, for (figure.8b), the order of dominant factors are as following: (rot) and (wel*wel).

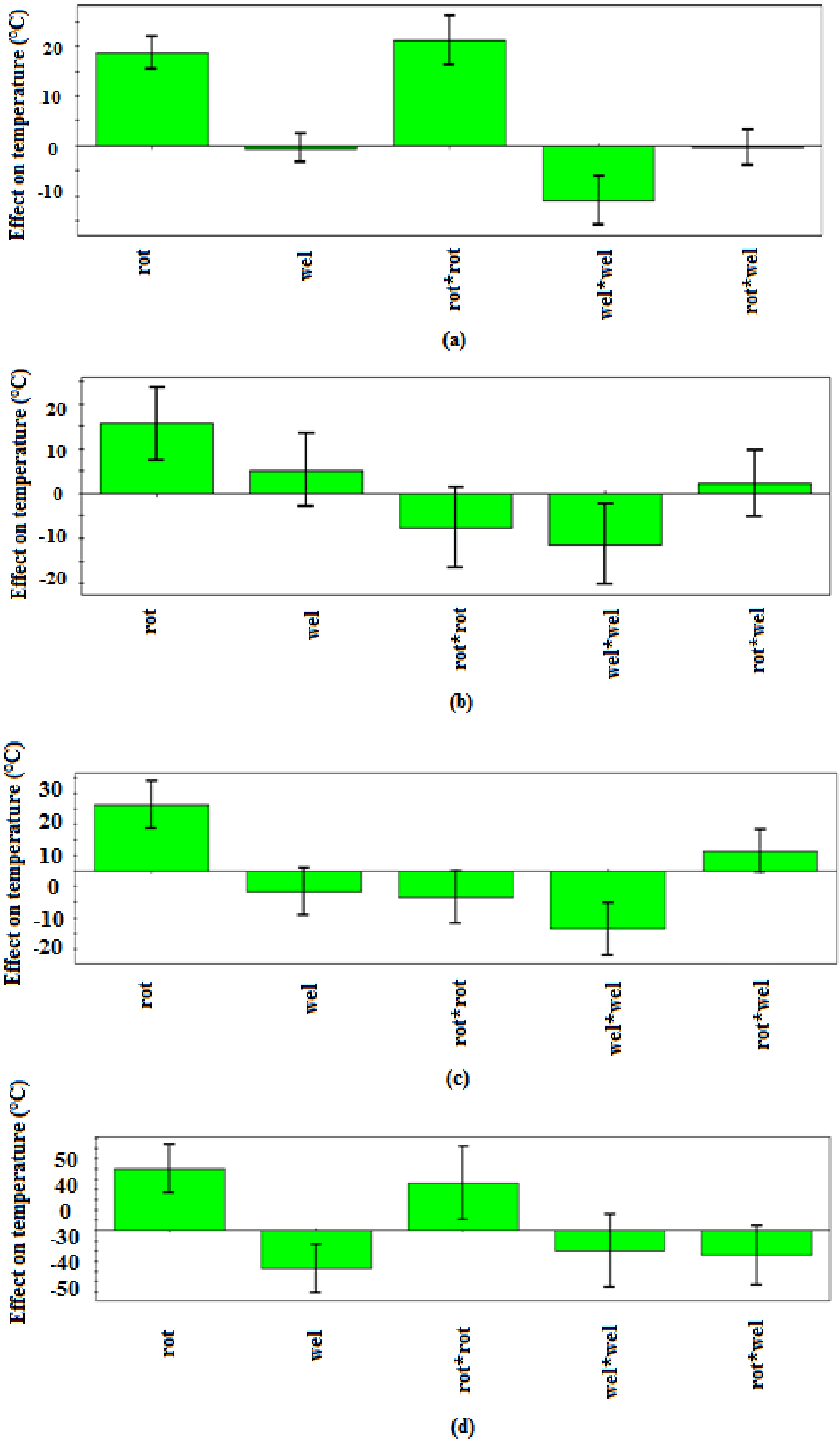

Figure 8. Effects of factors on temperature and their interaction, a) configuration A (lap joint), b) configuration B (lap joint), c) configuration A (Double lap joint), d) configuration B (Double lap joint

Sensitivity analysis, a method to identify critical parameters and rank them by their order of importance, is paramount in model validation where attempts are made to compare the calculated output with the measured data (Rajakumar et al, 2009).

Microhardness Measurements

The figure 9 shows the evolution of the hardness by defeating the speed of advance (160,200,250) mm/min and even the speed of rotation (1400 rpm), in both forms (single lap and double lap) on a SHIMADZU HMV-2000. In the hardness measurement, we used a load 1000g for 10 seconds per point and distance between the two points was 2mm along 28mm in hardness Vickers (HV).

The value of the stiffness in areas HAZ, TMAZ and NZ decreases from the value in BM due to the decrease in the displacement density resulting from FSW. We notice from the figure 9 that the value of the hardness decreases from the area HAZ in a direction TMAZ in various measurements until it reaches a minimum value and then rises in a direction NZ and this is due to the recrystallization of the grains because of the welding process (Abdulrehman et al, 2020). We also note a slight decrease in hardness value in the area NZ with an increase in welding speed (Merzoug et al, 2018). The hardness in the welded region is significantly lower with respect to the base material (50 μHV for single lap, 48 μHV for double lap). The high temperature achieved during the FSW process can be considered as the major cause of this softening effect. Even just a few microhardness values are reported for reasons of synthesis, it is possible to assert that the width of the softened region and the microhardness values recorded in the same region are influenced by the welding process parameters (D'Urso et al,, 2017).

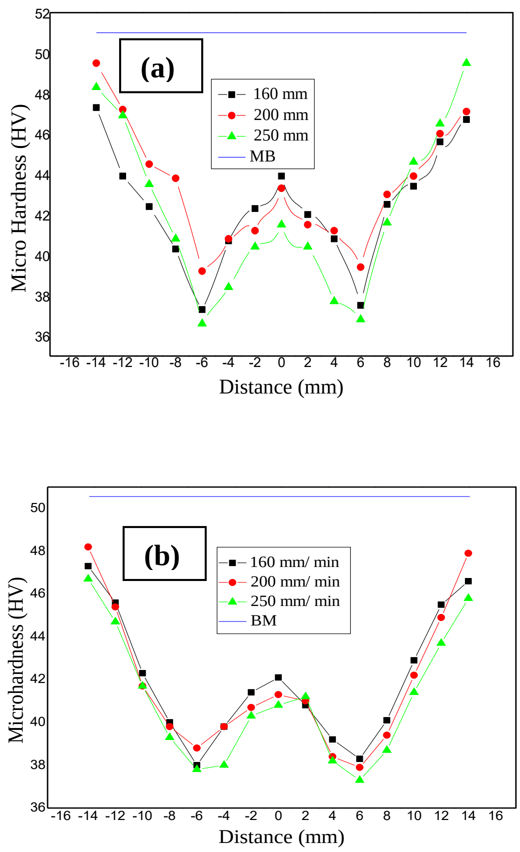

Figure 9. Hardness distribution profiles, a) Single lap, b) Double lap

Tensile Strength Test

We measured the tensile properties on the single and double lap in both configuration (A and B) are presented in figure 10 and figure 11, using constant tool rotation speeds of 1000 rpm (figure a), 1400 rpm (figure b), 2000 rpm (figure c), and tool displacement speeds of 160, 200 and 250 mm/min. To analyze the evolution of the mechanical with the welding parameters, averaged over several trials is calculated.

The results were presented according to the same parameter's to highlight the differences mechanical resistance of the two configurations (A and B). Figure 10 shows some representative curves, this figure shows that the load is maximum when the welding speed is equal to 160 mm/min (configuration B) Where the advancing side (AS) of the joint bore the main load, they reach a low value for a welding speed equal to 250 mm/min and rotation 1400 rpm (figure 10-b).

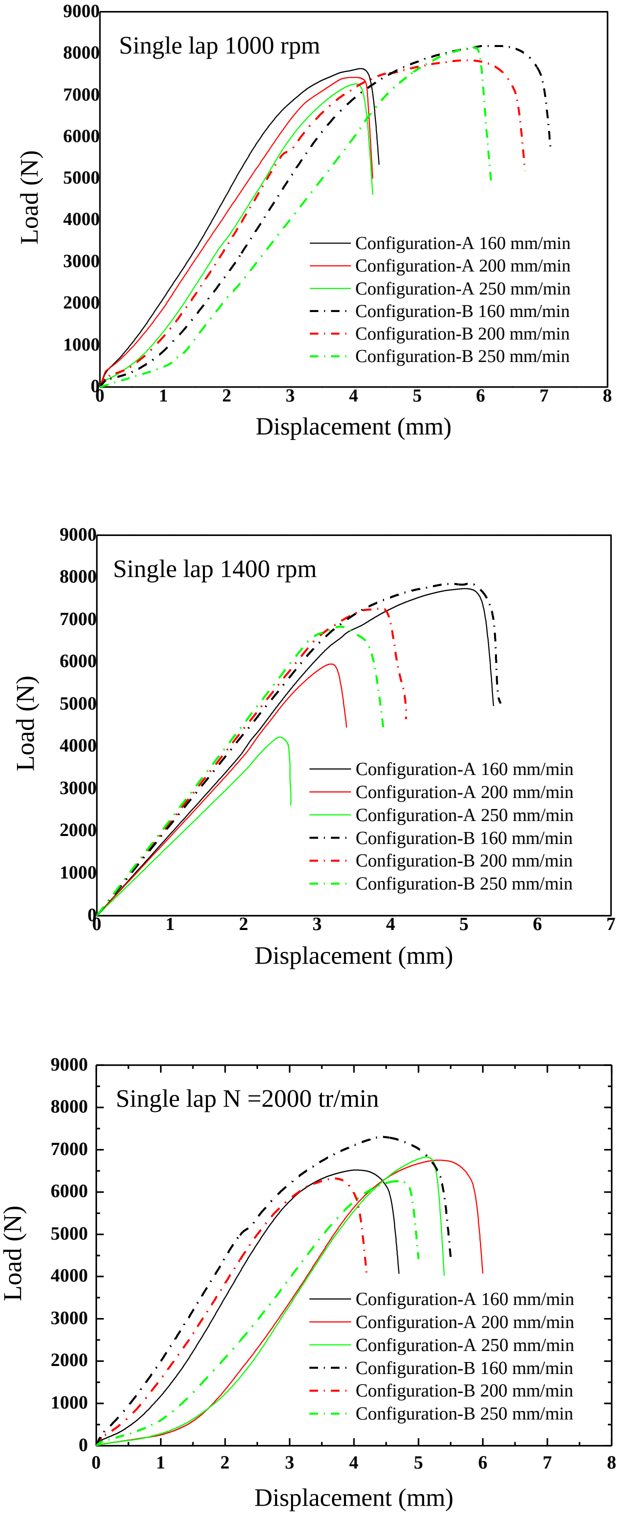

Figure 10. Load curve – displacement (single lap)

The load-displacement curve showed that the joint made at 1000 rpm possessed bigger displacement. Overall, for the configuration (B) the joint tensile shear performance was excellent. The same combination of parameters is shown in figure 11 for the double lap joint. It clearly indicates that with increasing travel speed for a constant rpm, failure load decreases for both the three cases (figures 11a, 11b and 11c). It is interesting to note that failure load of the joint can reach as high as 9000N. Through the plots the two figures, it can be seen that the double lap welds are having better tensile properties single lap welds.

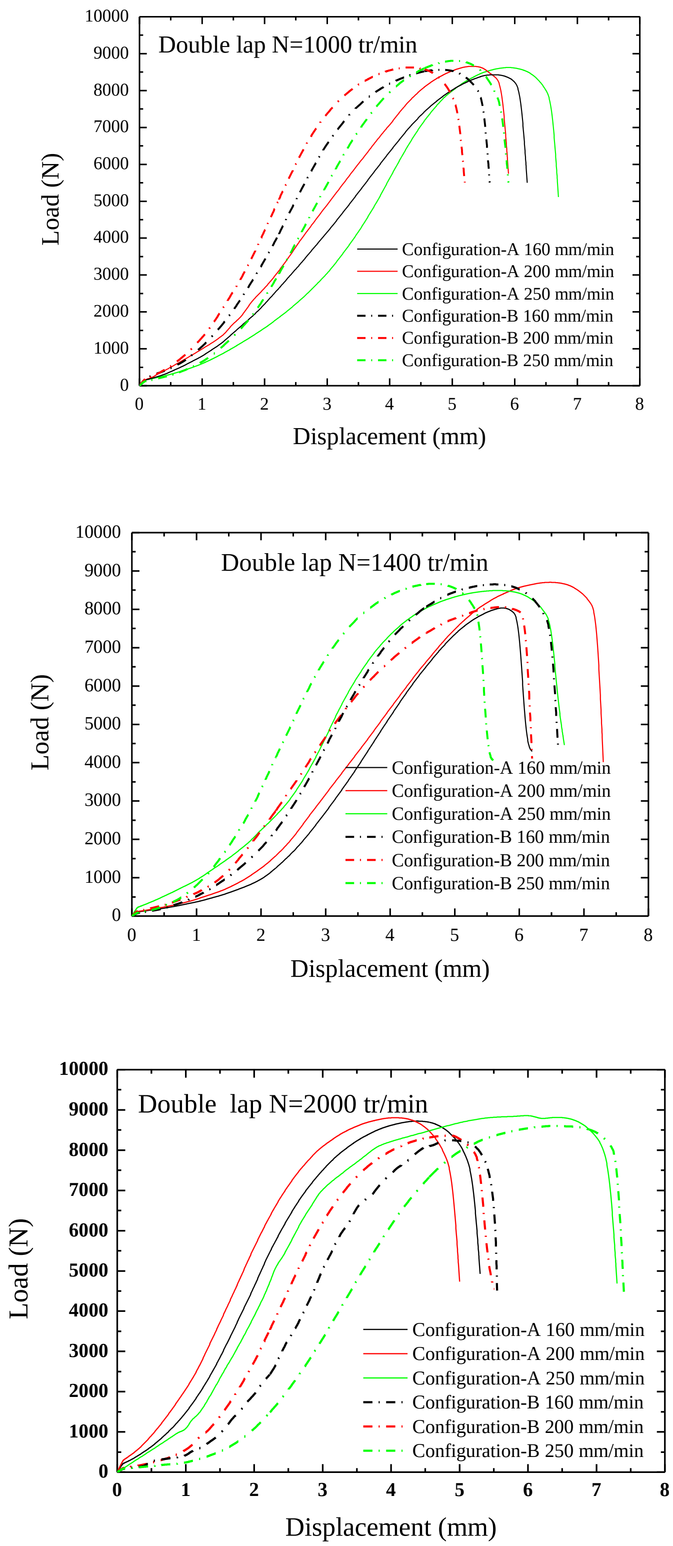

Figure 11. Load curve – displacement (double lap)

(a)

(b)

Figure 12. Specimens after tension test, a) single lap, b) double lap

Figure 12 groups the specimens after the tension test. It can be observed that final fracture is perpendicular to the loading direction in the center of the welded joint. On the test fractures of sheared samples one can see that for the lower linear welding speed a destruction (cracking) occurs along the plane passing through the weld and result in disruption of the joined elements. The fracture surfaces broken in this way, two characteristic zones can be seen in the weld area, i.e. a bright zone, which occurs on the advancing side of weld, and the darker area, which is visible in the retreating side of weld. The presence of such an area on the retreating side of joint is due to insufficient dispersion of oxides from the surfaces, which are only rubbed into weld area and form strongly adherent layer, thus reduces the mechanical properties of the joint (Krasnowski, 2014).

Conclusion

The present work was designed to identify the most influential and optimal friction stir welding process parameters on joint strength during FSLW welding of aluminium alloy AA3003. This study focuses on the influence of three factors (speed, feed rate, welding time). In particular the changes in microstructure, micro-hardness, and tensile properties of were investigated. It was found that the welding process treatment induces higher microhardness values and lower longitudinal residual stress in the weld zone surface. The flow material is facilitated around the tool pin while the surface hardness is improved at the same time.
The important conclusions are derived from this study are:

• For aluminium 3003 alloy welds, fracture strength was found to be very sensitive to pin positioning during FSLW.
• A maximum failure load of 9000 N was exhibited by the FSLW joints (double lap) fabricated with the optimized parameters of 1000 tr/min rotational speed, 250 mm/min welding speed. Also, this value (fractured at SZ) for the pin penetrated welds is itself higher than the maximum value (fractured at the SZ or interface) reported in literature when pin penetrating condition used.
• Beyond the HAZ, it can be seen that the stresses gradually tend towards zero when passing through the HAZ zone.

Scientific Ethics Declaration

The authors declare that the scientific ethical and legal responsibility of this article published in EPSTEM journal belongs to the authors.

Acknowledgements

* This article was presented as an oral presentation at the International Conference on Technology, Engineering and Science (www.icontes.net) held in Antalya/Turkey on November 16-19, 2022.

References

Abdulrehman, M. A., Challoob, S. H., & Marhoon, I. I. (2020). Investigation of mechanical and numerical properties of friction stir welding (FSW) for 3003-H14 aluminum alloys, In *Defect and diffusion forum. Trans. Tech. Publications Ltd*, *398*, 106-116.

Aydin, H., Tutar, M., Yigit, K., & Bayram, A. (2017). Mechanical properties of friction stir welded 3003 aluminum alloy in different welding conditions. *International Journal of Mechanical and Production Engineering*, *5*, 92-96.

Aydin, H. (2010). Quality and properties of the friction stir welded AA2024-T4 aluminum alloy at different welding conditions. *Materials Testing-Materials and Components Technology, 52,* 640-650.

Balasubramanian, V. (2014). Relationship between base metal properties and friction stir welding process parameters, *Materials Science and Engineering. A., 480* (1–2), 293–299.

Barekatain, H., Kazeminezhad, M., & Kokabi, A. H. (2014). Microstructure and mechanical properties in dissimilar butt friction stir welding of severely plastic deformed aluminum AA 1050 and commercially pure copper sheets. *Journal of Materials Science and Technology*, *30*, 826–834.

Birol, Y., & Kasman, S. (2013a). Effect of welding parameters on the microstructure and strength of friction stir weld joints in twin roll cast en AW Al-Mn1Cu plates. *Journal of Materials Engineering and Performance*, *22*(10), 3024-3033.

Birol, Y., & Kasman, S. (2013b). Friction stir welding of twin-roll cast en AW 3003 plates. *Metals and Materials International*, *19*(6), 1259–1266.

Buffa, G., Fratini, L., & Palmeri, D. (2006). On microstructural phenomena occurring in friction stir welding of aluminium alloys. *Journal of Materials Processing Technology*, *177* (1–3), 340–343.

Chen, C. M., & Kovacevic, R. (2003). Finite element modeling of friction stir welding—thermal and thermomechanical analysis. *International Journal of Machine Tools and Manufacture*, *43*(13), 1319-1326.

D'Urso, G.A., Giardini, C.A., Lorenzi, S.B., Cabrini, M.B., & Pastore, T.B. (2017). The Effects of process parameters on mechanical properties and corrosion behavior in friction stir welding of aluminum alloys. *17th International Conference on Sheet Metal, 2017, SHEMET17, Procedia Engineering*, *183*, 270 –276.

Elangovan, K., & Balasubramanian, V. (2007). Influences of pin profile and rotational speed of the tool on the formation of friction stir processing zone in AA2219 aluminium alloy. *Materials Science and Engineering A*., *459* (1–2), 7–18.

Kadaganchi, R., Gankidi, M. R., & Gokhale, H. (2014). Optimization of process parameters of aluminum alloyAA 2014-T6 friction stir welds by response surface methodology. *Defence Technology*, *11*, 209-219.

Krasnowski, K. (2014). Fatigue and static properties of friction stir welded aluminium alloy 6082 lap joints using triflute-type and smooth. *Archives of Metallurgy and Materials, 59*(1), 157-162. doi:10.2478/amm-2014-0025.

Merzoug, M.; Boulenouar, A.; Bouchouicha, B.; Serrier, M.; & Mazari, M.. (2018). Effects of welding parameters on fssw: experimental and numerical study, *Archives of Metallurgy and Materials*, *63*(1), 247-256. doi: 10.24425/118935.

Mishra, R. S., & Ma, Z. Y. (2005). Friction stir welding and processing. *Materials Science and Engineering*, *50* (2), 1-78.

Naik, B. S., Chen, D. L., Cao, X., & Wanjara, P. (2013). Microstructure and fatigue properties of a friction stir lap welded magnesium alloy. *Metallurgical and Materials Transactions A*, *44*(8), 3732-3746. doi: 10.1007/s11661-013-1728-5.

Rajakumar, S., Muralidharan, C., & Balasubramanian, V. (2010). Optimization of the friction-stir-welding process and tool parameters to attain a maximum tensile strength of AA7075–T6 aluminium alloy. *Proceedings of the Institution of Mechanical Engineers, Part B: Journal of Engineering Manufacture*, *224*(8), 1175-1191. doi:10.1243/ 0954405054JEM1802.2009.

Threadgill, P. L., Leonard, A. J., Shercliff, H. R., & Withers, P. J. (2009). Friction stir welding of aluminium alloys. *International. Materials. Reviews*, *54* (2), 49-93.

Tutar, M., Aydin, H., Yuce, C.,Yavuz, N., & Bayram, A. (2014). The optimisation of process parameters for friction stir spot- welded AA3003-H12 aluminium alloy using a Taguchi orthogonal array. *Material and Design*. *63*, 789-797.

Wiedenhoft, A. G., Amorim, H. J. D., Rosendo, T. D. S., Tier, M. A. D., & Reguly, A. (2018). Effect of heat input on the mechanical behaviour of Al-Cu FSW lap joints. *Materials Research*, *21*(4): e20170983

Xue, P., Ni, D. R., Wang, D., Xiao, B. L., & Ma, Z.Y. (2011). Effect of friction stir welding parameters on the microstructure and mechanical properties of the dissimilar Al–Cu joints. *Materials Science and Engineering A.,528*, 4683-4689.

Author Information

Mohamed MERZOUG
Materials and Reactive Systems Laboratory,
Mechanical Engineering Department,
Djillali Liabes University of Sidi-Bel-Abbes (22000),
BP. 89, City Larbi Ben Mhidi, Algeria
Email: m_merzoug01@yahoo.fr

Abdelatif MIMMI
Materials and Reactive Systems Laboratory,
Mechanical Engineering Department,
Djillali Liabes University of Sidi-Bel-Abbes (22000),
BP. 89, City Larbi Ben Mhidi, Algeria

Abdelkader GHAZI
Materials and Reactive Systems Laboratory,
Mechanical Engineering Department,
Mustapha Stambouli University of Mascara (29000),
Algeria.

To cite this article:

Merzoug, M., Mimmi, A., & Ghazi. A. (2022). Study of the correlation between the process parameters and the mechanical characteristics of the aluminum sheets welded by the FSW process. *The Eurasia Proceedings of Science, Technology, Engineering & Mathematics (EPSTEM), 21*, 335-348.